Generator coordinate method for 1D contacting bosons in harmonic trap

Jing-An Sun
Institute of Modern Physics, Fudan University, shanghai 200433, China

Guang-Jie Guo
Institute of Physics and Electronic Engineering, Xingtai University, Xingtai 054001 and Xingtai Key Laboratory for Research and Application of Robot Intelligent Detection and Sorting Technology, Xingtai University, Xingtai 054001, China)

Bo Zhou*
Key Laboratory of Nuclear Physics and Ion-Beam Application (MoE), Institute of Modern Physics, Fudan University, Shanghai 200433, China and Shanghai Research Center for Theoretical Nuclear Physics, NSFC and Fudan University, Shanghai 200438, China

Yu-Gang Ma†
Key Laboratory of Nuclear Physics and Ion-beam Application (MOE), Institute of Modern Physics, Fudan University, Shanghai 200433, China and Shanghai Research Center for Theoretical Nuclear Physics, NSFC and Fudan University, Shanghai 200438, China

(Dated: April 17, 2023)

We propose a new method, termed GCM-CPWF, for studying one-dimensional bosons confined in harmonic potentials with contact repulsive interactions. Our approach involves using the effective correlated pair wave function (CPWF) [PhysRevLett.108.045301] as a basis, combined with the generator coordinate method (GCM) to handle complex many-particle correlations accurately. We demonstrate the reliability of our GCM-CPWF wave functions by comparing ground energy and one-body density with those obtained by other numerical methods. Moreover, we present the energy spectrum up to six particles and the occupation number on the harmonic oscillator state. Utilizing these GCM-CPWF wave functions, we explore the properties of the ground and excited states of the many-particle system. Our GCM-CPWF framework is highly flexible and can be generalized to investigate more complex many-particle systems.

I. INTRODUCTION

Ultracold quantum gases are considered an ideal platform for simulating many-body systems with interactions due to the tunability of coupling strength and the feasibility of confinement techniques for atoms in a given potential [1, 2], which has attracted great attention [3–5]. The Tonks-Girardeau gas [6], where infinite repulsion interaction between contacting bosons maps to noninteracting fermions, and the super Tonks-Girardeau gas [7], which exhibits highly attractive excited states, are both experimentally observed. In addition to the experimental progress, several theoretical models have been developed to explore these novel quantum phenomena arising from many-body physics [8–12].

A typical many-body model is the one-dimensional bosonic gas in a harmonic trap with contact repulsive interaction, which is easily realizable experimentally and allows for the adjustment of interaction strength to any desired value, providing the opportunity to reveal fundamental properties of many-body systems. It is worth noting that this many-body model lacks a general analytical solution, which has prompted significant numerical and theoretical efforts to understand the experimental phenomena and gain insights into the model. Various methods have been proposed, including exact diagonalization [13], multi-configuration time-dependent Hartree method (MCTDH) [14], quantum Monte Carlo [15], tensor networks [16], artificial neural networks [17], and others. It should be noted that some methods actually restrict their applicability to specific situations, such as low dimensions, particular interaction regimes, and a small number of particles. For example, the computational cost of MCTDH grows exponentially with the number of degrees of freedom, and for $N = 5$ particles, 15 orbitals and 7.6×10^5 configurations are required [18].

* zhou_bo@fudan.edu.cn
† mayugang@fudan.edu.cn

In Ref. [19], starting from the analytical solution to two-body relative motion, the authors construct a many-body wave function according to exchange symmetry, which is called the correlated pair wave function (CPWF). The effectiveness of the CPWF has also been demonstrated in Ref. [19]. As we know, the generator coordinate method (GCM) [20–24] has been widely applied as a general many-body approach in the field of many-body physics. The key to the GCM is the selection of an effective basis, and the CPWF could serve as a suitable basis within the GCM framework for the accurate description of one-dimensional bosonic gas. In this article, we propose the new approach GCM-CPWF and apply it to study the many-particle system.

This paper is organized as follows. In Sec. II, we provide the details of the model and GCM-CPWF method. In Sec. III, our results are presented and compared with results from other numerical methods and a single CPWF for ground energy and density. The energy spectrua up to the first excited state for $N = 3, 4, 5, 6$ particles are also shown. To demonstrate the difficulty of approaching the real wave-function of this model using harmonic states, the occupation number distribution is presented. Finally, we make a summary and give the main conclusions of our work in Sec. IV.

II. MODEL AND METHOD

We will focus our attention on the one-dimensional contact-interacting bosonic system, which has been confined within a harmonic potential. In order to facilitate the calculation, we express the Hamiltonian of this model in dimensionless form,

$$H = -\frac{1}{2}\sum_{i=1}^{N}\frac{\partial^2}{\partial x_i^2} + \sum_{i=1}^{N}\frac{x_i^2}{2} + g\sum_{i<j}\delta(x_i - x_j), \tag{1}$$

where x_i is the position of i-th particle, N is the number of particles, g is the strength of contact interaction between bosons. The Hamiltonian can be separated into two parts, i.e., the center-of-mass part and the relative motion part, $H = H_{\text{c.m.}} + H_r$.

$$\begin{aligned} H_{\text{c.m.}} &= \frac{P^2}{2N} + \frac{NR^2}{2}, \\ H_r &= -\frac{1}{2N}\sum_{0<i<j\le N}\left(\frac{\partial}{\partial x_i} - \frac{\partial}{\partial x_j}\right)^2 \\ &\quad + \frac{1}{2N}\sum_{0<i<j\le N} x_{ij}^2 + \sum_{0<i<j\le N} g\delta(x_{ij}). \end{aligned} \tag{2}$$

Where $R = \frac{1}{N}\sum_{i=1}^{N} x_i$, $P = -i\sum_{i=1}^{N}\frac{\partial}{\partial x_i}$, and $x_{ij} = |x_i - x_j|$ represents the distance of each pair. The center-of-mass wave-function with respect to $H_{\text{c.m}}$ is $\Psi_R = \exp(-NR^2/2)$. Solving the many-body relative wave-functions in Eq. (2) is our main task.

Though there is no general analytical solution for the model above, an exact solution has been provided in the case of two particles [25], whose relative part is parabolic cylinder functions D_μ [26]. In Ref. [19], the CPWF for the relative motion of N particles is constructed based on the pair function, which reads

$$\Psi_{\text{CP}}(\beta) = \prod_{0<i<j\le N} D_\mu(\beta x_{ij}), \tag{3}$$

where β and μ are parameters satisfied in the following equation,

$$\frac{g}{\beta} = -\frac{2^{3/2}\Gamma(\frac{1-\mu}{2})}{\Gamma(-\frac{\mu}{2})}. \tag{4}$$

This equation is determined by the boundary condition $2\beta D_{ij}(0) = gD_{ij}(0)$, where $D'_{ij} = \frac{\partial D_{ij}}{\partial(\beta x_{ij})}$ and $D_{ij} = D_\mu(\beta x_{ij})$.

Regarding the constructed Ψ_{CP} wave function presented above, it is worth noting that for the case of $N = 2$, this wave function is reduced to the analytical solution to the two-body relative motion. When extended to systems with more particles, the Ψ_{CP} wave functions have been proven to be effective in describing the system in comparison to other computational methods. However, it should be emphasized that the Ψ_{CP} wave function with $\beta = \sqrt{2/N}$ may not yield highly accurate numerical solutions for larger values of N and for broad contact interaction strengths.

In Ref. [19], β is considered as variable parameters. To achieve a more precise description of bosonic systems with a greater number of particles, we propose treating β as the generator coordinate. This approach allows for the construction of a more general many-body wave function for relative motion by superposing multiple $\Psi_{\rm CP}$ wave functions with varying β values,

$$\Psi_{\rm rel}(\boldsymbol{x}) = \sum_{\beta_i} C_{\beta_i} \Psi_{CP}(\beta_i), \tag{5}$$

where C_{β_i} are coefficients to be determined. The whole wave-function reads $\Psi(\boldsymbol{x}) = \Psi_R \Psi_{\rm rel}$. To get the solution, the Hill-Wheeler equation should be solved,

$$\sum_{\beta_j} [H(\beta_i, \beta_j) - EN(\beta_i, \beta_j)] C_{\beta_j} = 0 \tag{6}$$

where

$$H(\beta_i, \beta_j) = \int \Psi_R^*(\boldsymbol{x}) \Psi_{CP}^*(\beta_i) H \Psi_R(\boldsymbol{x}) \Psi_{CP}(\beta_j) \mathrm{d}\boldsymbol{x}, \tag{7}$$

$$N(\beta_i, \beta_j) = \int \Psi_R^*(\boldsymbol{x}) \Psi_{CP}^*(\beta_i) \Psi_R(\boldsymbol{x}) \Psi_{CP}(\beta_j) \mathrm{d}\boldsymbol{x}, \tag{8}$$

which are called Hamiltonian kernels and normal kernels, respectively.

For the model above, the normal kernels and Hamiltonian kernels can be calculated as below. Notice that,

$$\begin{aligned}
H_r \Psi_{\rm CP} &= \sum_{i<j}^{P} \delta(r_{ij}) \left(-2\beta D'_{ij} + g D_{ij}\right) \phi^{ij} - \beta^2 \sum_{i<j}^{P} \left(D''_{ij} - \frac{(\beta r_{ij})^2}{4} D_{ij} \right) \phi^{ij} \\
&+ \frac{2 - N\beta^4}{4N} \sum_{i<j}^{P} x_{ij}^2 D_{ij} \phi^{ij} + \frac{\beta^2}{2} \sum_{k<l, p<q, kl \neq pq} \phi^{kl,pq} D'_{kl} D'_{pq} \chi_{kl,pq} \\
&= \beta^2 (\mu + \frac{1}{2}) \sum_{i<j} D_{ij} \phi^{ij} + \frac{2 - N\beta^4}{4N} \sum_{i<j}^{P} x_{ij}^2 D_{ij} \phi^{ij} + \frac{\beta^2}{2} \sum_{k<l, p<q, kl \neq pq} \phi^{kl,pq} D'_{kl} D'_{pq} \chi_{kl,pq} \\
&= \beta^2 P (\mu + \frac{1}{2}) \Psi_{CP} + \frac{2 - N\beta^4}{4N} \sum_{i<j}^{P} x_{ij}^2 \Psi_{CP} + \frac{\beta^2}{2} \sum_{k<l, p<q, kl \neq pq} \phi^{kl,pq} D'_{kl} D'_{pq} \chi_{kl,pq}
\end{aligned} \tag{9}$$

where $\phi^{kl,pq} = \prod_{i<j(ij \neq kl,pq} D_\mu(\beta r_{ij})$ and

$$\chi_{kl,pq} = \begin{cases} 0 & k = p \quad \text{and} \quad l = q \\ \theta(x_k - x_l)\theta(x_p - x_q) & l = p \quad \text{or} \quad k = q \\ -\theta(x_k - x_l)\theta(x_p - x_q) & k = p \quad \text{or} \quad l = q \end{cases} \tag{10}$$

$\theta(x)$ is the sign function. Therefore, the normal kernel and Hamiltonian kernel between for the generator coordinate β_a and β_b can be written as,

$$N_{ab} = \langle \Psi(\beta_a) | \Psi(\beta_b) \rangle = \int d\boldsymbol{x} \Psi_R^2 \Psi_{CP}(\beta_a) \Psi_{CP}(\beta_b) \tag{11}$$

$$\begin{aligned}
H_{ab} &= \left(\frac{1}{2} + \beta^2 P (\mu + \frac{1}{2}) \right) N_{ab} + \frac{2 - N\beta^4}{4N} \sum_{i<j}^{P} \int d\boldsymbol{x} r_{ij}^2 \Psi_R^2 \Psi_{CP}(\beta_a) \Psi_{CP}(\beta_b) \\
&+ \frac{\beta^2}{2} \sum_{k<l, p<q, kl \neq pq} \int d\boldsymbol{x} \phi^{kl,pq}(\beta_b) D'_{kl}(\beta_b) D'_{pq}(\beta_b) \chi_{kl,pq} \Psi_R^2 \Psi_{CP}(\beta_a)
\end{aligned} \tag{12}$$

Thus, based on the obtained kernels and taking the proper meshpoints of the generator parameters $\{\boldsymbol{\beta}\}$, the GCM wave function in Eq. (5) can be obtained.

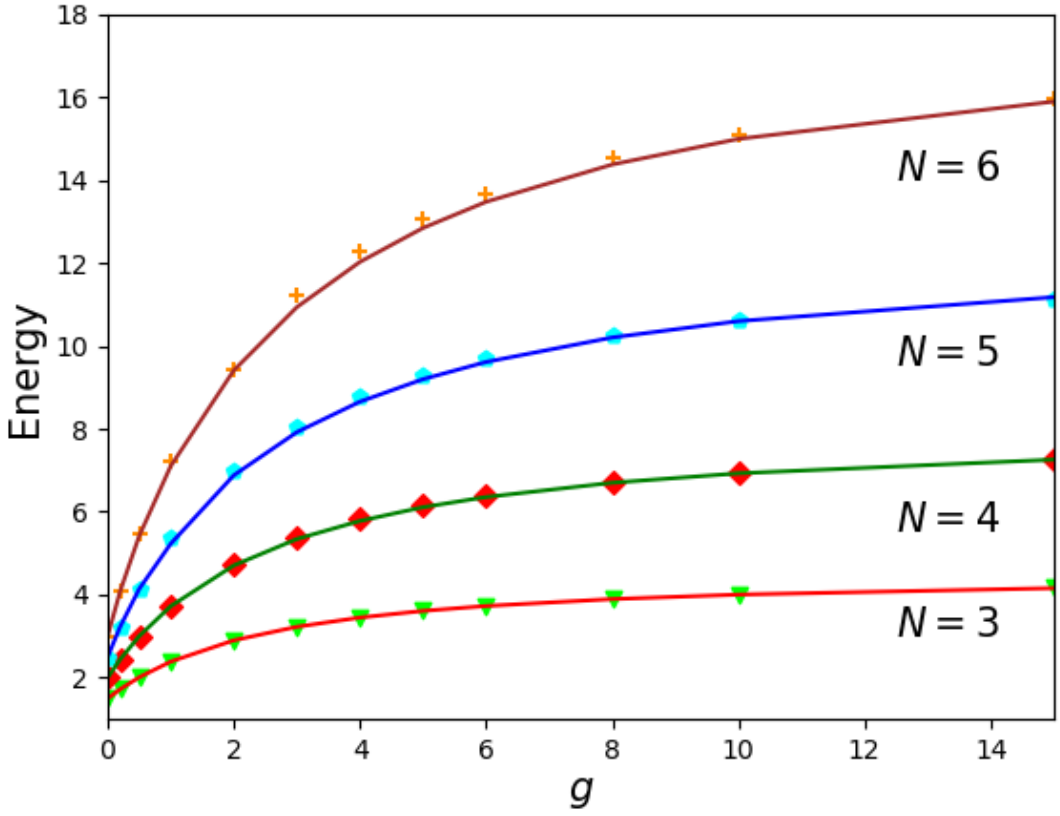

FIG. 1. Ground state energies as a function of the coupling strength g obtained from GCM-CPWF (lines) and wave-function where β is fixed at $\sqrt{2/N}$ (marks) for$N = 3, 4, 5, 6$

III. RESULTS AND DISCUSSIONS

In our study, we employ GCM-CPWF calculations by superposing several CPWF basis wave-functions with different β values. We begin by noting that the ground state energies of several particles obtained through the single wave-function $\Psi_{\mathrm{CP}}(\beta = \sqrt{2/N})$ are consistent with advanced numerical methods like the exact diagonalization method and multiconfiguration time-dependent Hartree method. Therefore, we verify our GCM results by comparing them with the single wave-function $\Psi_{\mathrm{CP}}(\beta = \sqrt{2/N})$ for different particles as a function of interaction strength g.

Figure 1 illustrates the agreement between the energies calculated by the single wave-function $\Psi_{\mathrm{CP}}(\beta = \sqrt{2/N})$ and GCM-CPWF for different interaction strengths g up to $N = 6$ particles. Notably, the ground energies given by GCM-CPWF are consistently slightly lower than those from the single wave-function ($\beta = \sqrt{2/N}$) and other numerical methods, indicating that GCM-CPWF offers more accurate descriptions of ground states for various particle numbers. At weak and strong coupling strengths, the methods show good agreement, yielding relative accuracy on the order of 10^{-3}. However, at intermediate coupling strengths, particularly for $N = 5, 6$ particles, some deviation is observed, leading to an agreement of 10^{-1}.

To further verify the accuracy of the GCM-CPWF wave functions obtained, we compare the one-body density functions $\rho(x)$ calculated by the single wave functions and GCM-CPWF wave functions in Fig. 2. It is shown that the $\rho(x)$ obtained by the GCM-CPWF and Ψ_{CP} wave functions agree well with each other in the strong and weak interaction regimes. This suggests that our GCM-CPWF results are consistent with other numerical results, as the Ψ_{CP} wave functions have been shown to be accurate in the two-limit interaction regions in Ref. [19].

However, a significant discrepancy is observed at intermediate g, where the calculated densities from GCM-CPWF have a narrower shape and longer tail than those from the single $\Psi_{\mathrm{CP}}(\beta = \sqrt{2/N})$ wave functions. If β was treated as a variational parameter in the $\Psi_{\mathrm{CP}}(\beta)$ function, the calculated densities could be closer to our GCM results, as shown in Fig. 2 for $g = 2$.

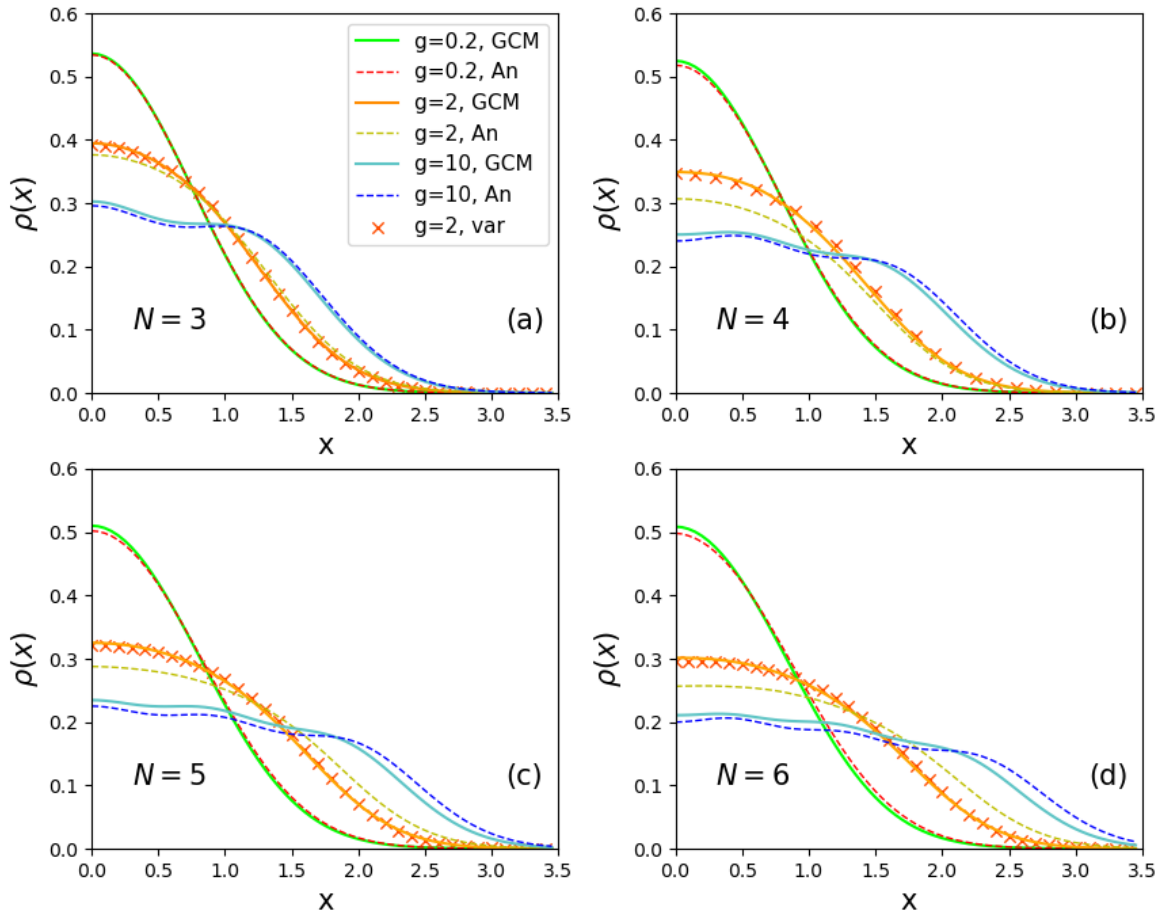

FIG. 2. One-body densities obtained from single wave-function and GCM-CPWF for (a) $N = 3$, (b) $N = 4$, (c) $N = 5$, (d) $N = 6$ at $g = 0.2, 2, 10$. The variational results for $g = 2$ are also presented in plots.

In a recent paper [27], the authors developed a direct diagonalization method to calculate the ground energy and density function for the same Hamiltonian we consider in this work. Their approach is to represent the many-body wave function in the Hilbert space spanned by the harmonic oscillator states (HOS). However, the dimension of the Hilbert space becomes highly large, making it difficult to obtain the exact many-body wave function. To tackle this issue, they use energy truncation to reduce the number of configurations. For instance, when they consider 4 particles and 20 single HOS, the dimension of the Hilbert space is reduced from 4100,625 to 194,580 after energy truncation. Although the effectiveness of the energy truncation has been demonstrated, it still requires many HOS and is difficult to generalize to more particles.

In our work, we perform GCM-CPWF calculations by superposing several CPWF basis wave functions with different β. In Fig. 3, we compare the one-body density functions from GCM and the direct diagonalization method at $g = 5$ for $N = 2, 3, 4, 5, 6$. We observe a high level of agreement between the two methods for $N = 2, 3, 4$, while for $N = 5, 6$ there is a slight discrepancy with the density functions from GCM-CPWF having narrower shapes and longer tails. Notably, we use no more than 10 basis wave functions in our method, whereas the direct diagonalization method requires at least 100 thousand HOS basis wave functions.

The GCM-CPWF framework not only provides more precise ground energy and density estimates, but also facilitates the exploration of excited states. As is well known, the excited states cannot be studied solely based on the single $\Psi_{\rm CP}$ wave function. Figure 4 displays the energy spectrum as a function of coupling strength up to the first excited state for $N = 3, 4, 5, 6$ particles. It is observed that the first excited energies rise rapidly for weak coupling strength

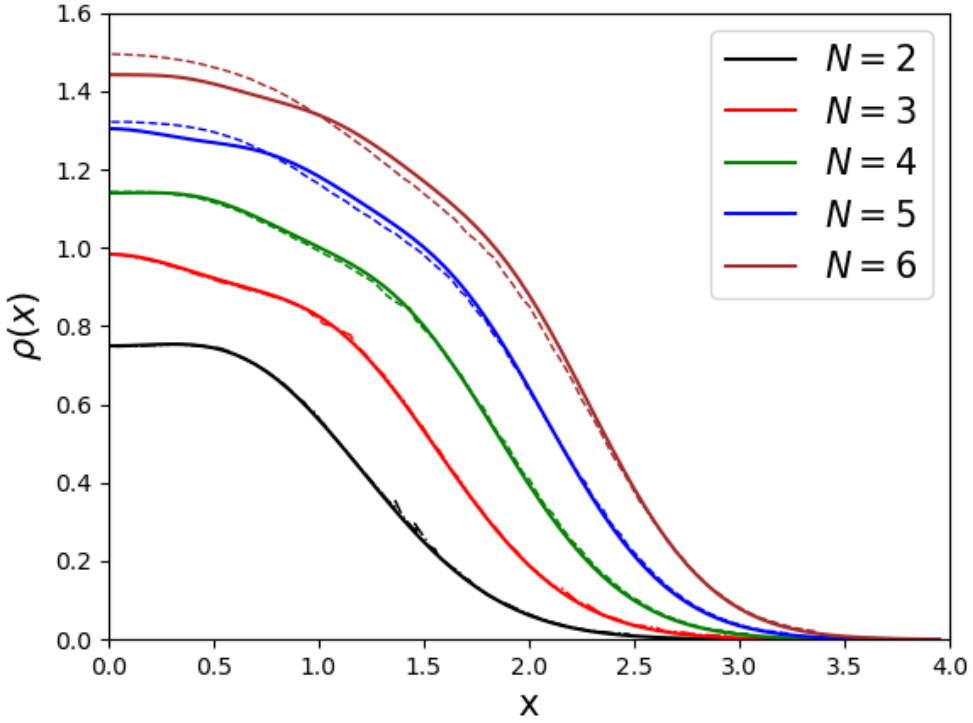

FIG. 3. One-body ground density functions from GCM-CPWF and corrected direct diagonalization in [27] for $N = 2, 3, 4, 5, 6$ at $g = 5$.

and gradually saturate as g increases. Interestingly, in the range of $g > 0.5$, the energy gap between excited energy and ground energy remains almost constant, that is, $\Delta \sim 1.85$.

Figure 5 presents the ground and first excited one body density functions $\rho(x)$ for $g = 5$ when $N = 3, 4, 5, 6$. Clearly, the first excited density exhibits an apparent expansion, characterized by a longer tail and wider shape. More intriguingly, at intermediate g, the density of the first excited state flattens and forms a peak structure compared to the ground state, whose one body density function lacks a peak. For the ground state, the peak structure of the density function for strong interaction is attributable to fermionization, which reflects the tendency of atoms to repel each other under strong contact interaction and behave like fermions. However, the fermionization interpretation fails to explain the peak structure for the excited state, since the interaction is not strong enough to induce localization. It is because the bosons occupy higher energy levels, causing the bosons can appear in certain positions [28].

Finally, we turn our attention to the occupation numbers of harmonic oscillator states in the ground and the first excited states. The occupation number of the ith energy level of the harmonic oscillator is given by:

$$n_i = \int_{-\infty}^{\infty} \rho(x, x')\phi_i(x)\phi_i(x')dxdx'. \tag{13}$$

where $\phi_i(x)$ is the i-th Eigen-wavefunction of 1D harmonic oscillator and the one-body correlation function is defined as,

$$\rho(x, x') = \int \Psi(x, x_2, x_3, \ldots, x_N) \times \Psi(x', x_2, x_3, \ldots, x_N)\mathrm{d}x_2 \ldots \mathrm{d}x_N. \tag{14}$$

.

The occupation number distribution of 1D harmonic oscillator states is illustrated in Fig. 6. For the ground state of the six-boson system, a majority of the particles occupy the lowest energy level when the interaction strength is weak, and as the interaction strength increases, more particles occupy higher energy levels. Additionally, it can be

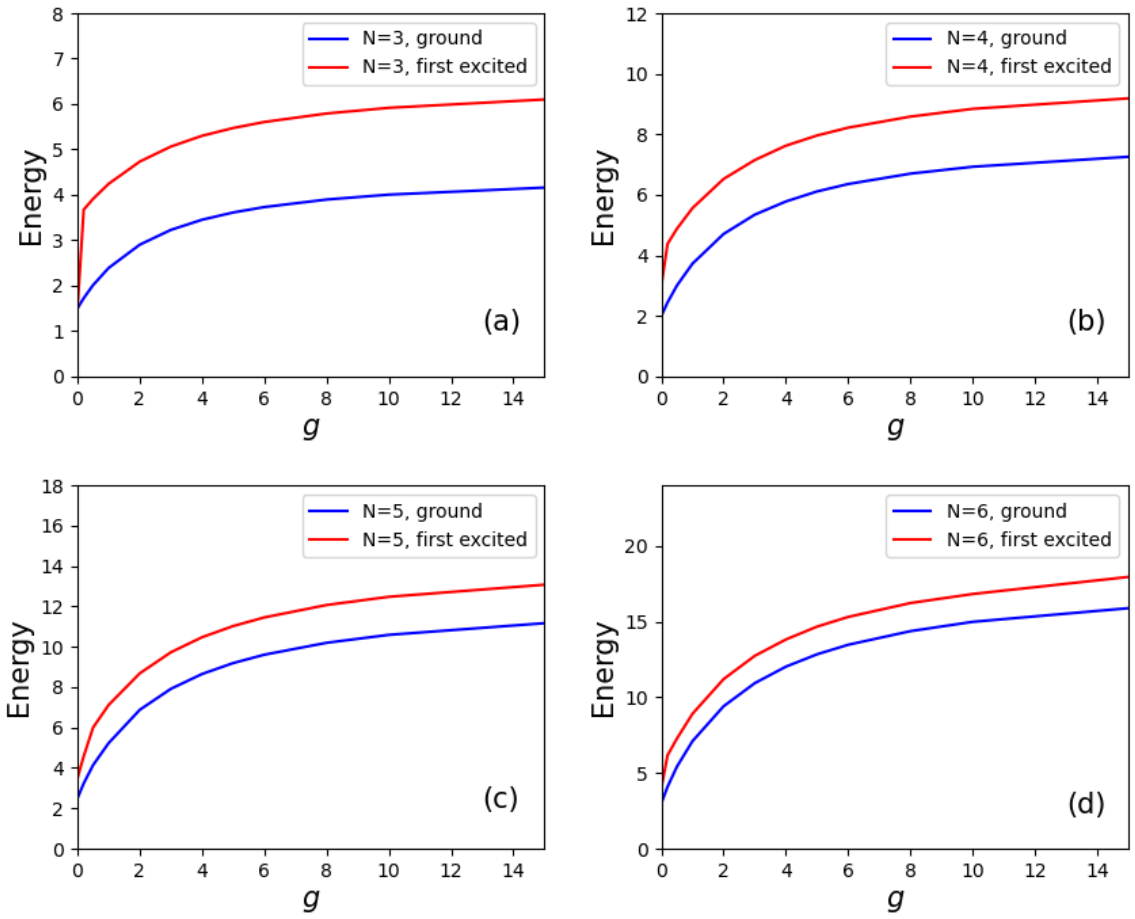

FIG. 4. Energy spectrum up to first excited state for (a) $N = 3$, (b) $N = 4$, (c) $N = 5$, (d) $N = 6$

observed that more energy levels are involved for stronger interactions. Moreover, the occupation of even energy levels is stronger than that of odd energy levels between neighboring levels, indicating a preference of the bosons for occupying even harmonic oscillator states as the interaction strength increases, as depicted in Fig. 6.

In contrast, for the first excited state of the system, the particles leave the lowest energy level and occupy higher energy levels. Moreover, more energy levels are occupied when the system is excited.

Returning to the peak structure of the excited state, the changes in the density function with respect to g can be interpreted as a rearrangement of particles on the harmonic oscillator states (HOS). For particles in the excited state at $g = 5$, they tend to occupy higher HOS and have more nodes than those in the ground excited state at $g = 5$. As a result, the one-body density function for the excited state at $g = 5$ exhibits a peak structure, whereas the ground density function has no peaks. Similarly, the ground one-body density function at $g = 15$ also exhibits peak structures due to the arrangement of particles on HOS. Interestingly, we observe that the arrangement of the excited state at $g = 5$ is quite similar to that of the ground state at $g = 15$.

Figure 6 reveals that at least seven harmonic oscillator states (HOS) are necessary to describe the single-particle behavior of the system. However, this does not imply that only seven HOS modes are sufficient to describe the wave function of the system. In reality, at least twenty HOS modes need to be considered, and there are $20^6 = 64,000,000$ states that need to be taken into account [27]. Even after truncation, there are still $177,100$ states. This suggests that the higher energy levels of the HOS can have a non-negligible impact on the exact wave functions, even if the occupation numbers of these levels are at the order of 10^{-3}. Therefore, to gain a comprehensive understanding of the 1D bosonic system with an increasing number of particles, it is challenging to rely solely on the HOS modes.

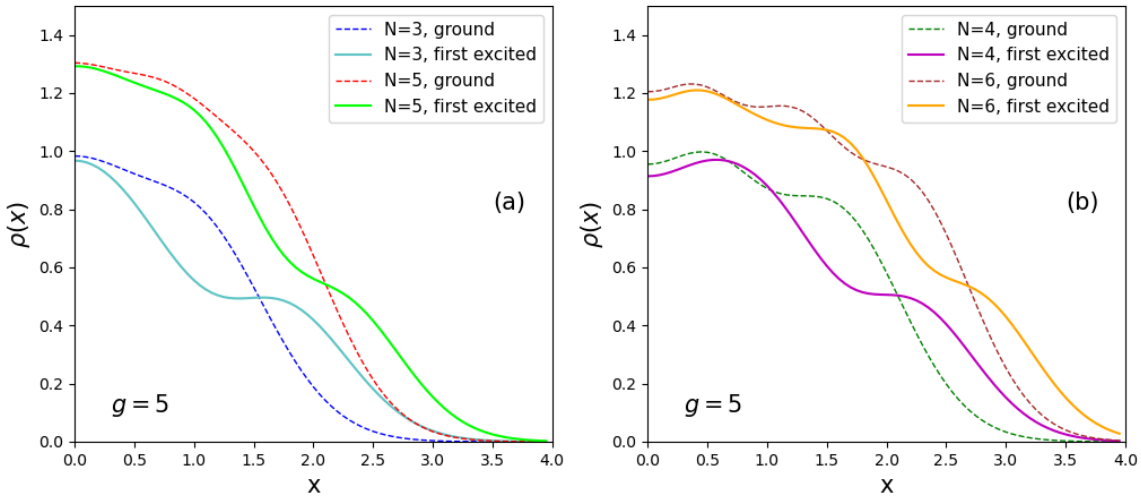

FIG. 5. The one-body density for ground and excited state at $g = 5$.

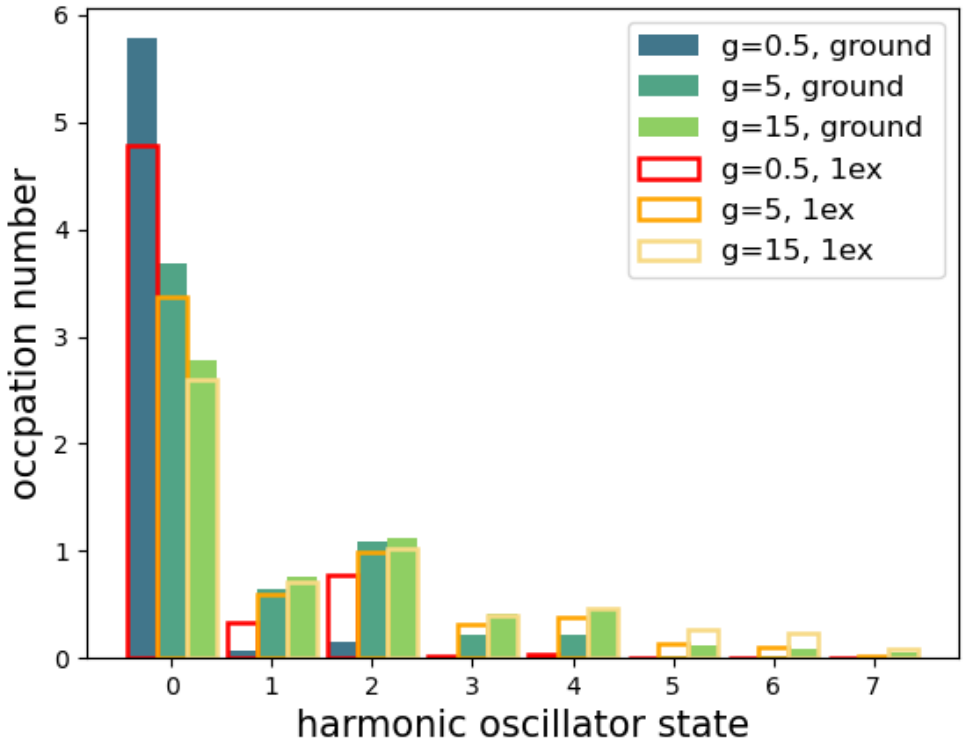

FIG. 6. Occupation numbers on harmonic oscillator states of N=6 bosons at $g = 0.5, 5, 15$ for ground and first excited states.

However, the GCM-CPWF framework developed in this work could facilitate the study of wave functions of few-body to many-body systems, provided we obtain the fundamental essence of the two-body correlation function, which will be our next focus.

IV. SUMMARY AND CONCLUSIONS

This paper introduces GCM-CPWF, a novel method for studying many-body systems, and applies it to a 1D bosonic system in a harmonic trap with contact repulsive interaction. The method involves treating the CPWF, which is constructed using two-body analytical correlation functions, as a generator state within the GCM formalism. By superposing generator states with varying parameters, denoted by β in this article, a general many-body wavefunction is obtained.

Using GCM-CPWF, we calculate the ground energy and one-body density function up to 6 particles and compare the results to those from other numerical methods. The approach is found to be accurate, with a ground energy error on the order of 10^{-3} and excellent consistency in the one-body density. Excited states of the model are also explored, revealing interesting behavior at different coupling strengths. Specifically, the first excited energy rises quickly for weak interaction and saturates for strong interaction, due to fermionization at strong coupling regimes. Interestingly, when the density of the ground state for intermediate interaction has no peak, the density of the excited state forms peaks at the same g. This can be understood by the fact that the boson has been promoted to a higher energy level in the excited state, leading it more likely to be found in certain regions of space.

We also consider the occupation number on harmonic oscillator states, finding that higher energy levels of HOS cannot be ignored when studying exact many-body wave functions, despite having negligible occupation numbers. This presents a challenge in studying wave functions from few-body to many-body, but the GCM-CPWF method shows potential in overcoming this difficulty by reducing many-body problems to two-body problems through a deep understanding of two-body correlations.

ACKNOWLEDGMENTS

This work was partially supported by the National Natural Science Foundation of China under Grant No. 12147101, No. 11890714, No. 12175042, Xingtai Young Talent Programme for Science and Technology with Grant No. 2018ZZ033, and Shanghai "Science and Technology Innovation Action Plan" Project No. 21ZR140950.

[1] I. Bloch, J. Dalibard, and W. Zwerger, Many-body physics with ultracold gases, Rev. Mod. Phys. **80**, 885 (2008).
[2] C. Chin, R. Grimm, P. Julienne, and E. Tiesinga, Feshbach resonances in ultracold gases, Rev. Mod. Phys. **82**, 1225 (2010).
[3] X.-C. Yan, D.-L. Sun, L. Wang, J. Min, S.-G. Peng, and K.-J. Jiang, Production of degenerate fermi gases of ^{6}li atoms in an optical dipole trap, Chinese Physics Letters **38**, 056701 (2021).
[4] S. Yang, T. Zhou, C. Li, K. Yang, Y. Zhai, X. Yue, and X. Chen, Superfluid-mott-insulator transition in an optical lattice with adjustable ensemble-averaged filling factors, Chinese Physics Letters **37**, 040301 (2020).
[5] Z.-C. Xu, Z. Zhou, E. Cheng, L.-J. Lang, and S.-L. Zhu, Gain/loss effects on spin-orbit coupled ultracold atoms in two-dimensional optical lattices, SCIENCE CHINA-PHYSICS MECHANICS & ASTRONOMY **65**, 10.1007/s11433-022-1898-7 (2022).
[6] B. Paredes, A. Widera, V. Murg, O. Mandel, S. Fölling, I. Cirac, G. V. Shlyapnikov, T. W. Hänsch, and I. Bloch, Tonks–girardeau gas of ultracold atoms in an optical lattice, Nature **429**, 277 (2004).
[7] E. Haller, M. Gustavsson, M. J. Mark, J. G. Danzl, R. Hart, G. Pupillo, and H.-C. Nägerl, Realization of an excited, strongly correlated quantum gas phase, Science **325**, 1224 (2009).
[8] D. Raventós, T. Graß, M. Lewenstein, and B. Juliá-Díaz, Cold bosons in optical lattices: a tutorial for exact diagonalization, Journal of Physics B: Atomic, Molecular and Optical Physics **50**, 113001 (2017).
[9] F. Dalfovo, S. Giorgini, L. P. Pitaevskii, and S. Stringari, Theory of bose-einstein condensation in trapped gases, Rev. Mod. Phys. **71**, 463 (1999).
[10] H.-D. Meyer and G. A. Worth, Quantum molecular dynamics: propagating wavepackets and density operators using the multiconfiguration time-dependent hartree method, Theoretical Chemistry Accounts **109**, 251 (2003).
[11] G. Carleo and M. Troyer, Solving the quantum many-body problem with artificial neural networks, Science **355**, 602 (2017).
[12] Y. Yang, H. Cao, and Z. Zhang, Neural network representations of quantum many-body states, SCIENCE CHINA-PHYSICS MECHANICS & ASTRONOMY **63**, 10.1007/s11433-018-9407-5 (2020).
[13] F. Deuretzbacher, K. Bongs, K. Sengstock, and D. Pfannkuche, Evolution from a bose-einstein condensate to a tonks-girardeau gas: An exact diagonalization study, Phys. Rev. A **75**, 013614 (2007).
[14] S. Zöllner, H.-D. Meyer, and P. Schmelcher, Ultracold few-boson systems in a double-well trap, Phys. Rev. A **74**, 053612 (2006).
[15] G. E. Astrakharchik and S. Giorgini, Correlation functions and momentum distribution of one-dimensional bose systems, Phys. Rev. A **68**, 031602(R) (2003).

[16] F. Verstraete, V. Murg, and J. I. Cirac, Matrix product states, projected entangled pair states, and variational renormalization group methods for quantum spin systems, Advances in physics **57**, 143 (2008).
[17] G. Carleo and M. Troyer, Solving the quantum many-body problem with artificial neural networks, Science **355**, 602 (2017).
[18] I. Brouzos and P. Schmelcher, Controlled excitation and resonant acceleration of ultracold few-boson systems by driven interactions in a harmonic trap, Phys. Rev. A **85**, 033635 (2012).
[19] I. Brouzos and P. Schmelcher, Construction of analytical many-body wave functions for correlated bosons in a harmonic trap, Phys. Rev. Lett. **108**, 045301 (2012).
[20] C. W. Wong, Generator-coordinate methods in nuclear physics, Physics Reports **15**, 283 (1975).
[21] P. Ring and P. Schuck, *The nuclear many-body problem* (Springer Science & Business Media, 2004).
[22] B. Zhou, A. Tohsaki, H. Horiuchi, and Z. Ren, Breathing-like excited state of the hoyle state in c12, Phys. Rev. C **94**, 044319 (2016).
[23] T. Ichikawa and N. Itagaki, Optimization of basis functions for multiconfiguration mixing using the replica exchange Monte Carlo method and its application to 12C, Phys. Rev. C **105**, 024314 (2022).
[24] X. Zhang, W. Lin, J. M. Yao, C. F. Jiao, A. M. Romero, T. R. Rodríguez, and H. Hergert, Optimization of the generator coordinate method with machine-learning techniques for nuclear spectra and neutrinoless double-β decay: Ridge regression for nuclei with axial deformation, Phys. Rev. C **107**, 024304 (2023).
[25] T. Busch, B.-G. Englert, K. Rzażewski, and M. Wilkens, Two cold atoms in a harmonic trap, Foundations of Physics **28**, 549 (1998).
[26] M. Abramowitz and I. A. Stegun, *Handbook of mathematical functions with formulas, graphs, and mathematical tables*, Vol. 55 (US Government printing office, 1964).
[27] A. Rojo-Francàs, F. Isaule, and B. Juliá-Díaz, Direct diagonalization method for a few particles trapped in harmonic potentials, Phys. Rev. A **105**, 063326 (2022).
[28] S. Zöllner, H.-D. Meyer, and P. Schmelcher, Excitations of few-boson systems in one-dimensional harmonic and double wells, Phys. Rev. A **75**, 043608 (2007).